Journal of
Plankton Research

academic.oup.com/plankt

J. Plankton Res. (2021) 43(2): 103–112. First published online March 17, 2021 doi:10.1093/plankt/fbab014

ORIGINAL ARTICLE

Phytoplankton carbon and nitrogen biomass estimates are robust to volume measurement method and growth environment

HEATHER MCNAIR[1,*], **COURTNEY NICOLE HAMMOND**[1,2,†] **AND SUSANNE MENDEN-DEUER**[1]

[1]UNIVERSITY OF RHODE ISLAND, GRADUATE SCHOOL OF OCEANOGRAPHY, 215 S FERRY RD., NARRAGANSETT, RI 02882, USA AND [2]SALISBURY UNIVERSITY, DEPARTMENT OF BIOLOGICAL SCIENCES, 1101 CAMDEN AVE., SALISBURY, MD 21801, USA

*CORRESPONDING AUTHOR: hmcnair@uri.edu

† PRESENT ADDRESS: LOUISIANA STATE UNIVERSITY, COLLEGE OF THE COAST AND ENVIRONMENT, 93 SOUTH QUAD DRIVE, SUITE 1002, BATON ROUGE, LA 70803, USA

Received October 23, 2020; editorial decision January 29, 2021; accepted February 1, 2021

Corresponding editor: Lisa Campbell

Phytoplankton biomass is routinely estimated using relationships between cell volume and carbon (C) and nitrogen (N) content that have been defined using diverse plankton that span orders of magnitude in size. Notably, volume has traditionally been estimated with geometric approximations of cell shape using cell dimensions from planar two-dimensional (2D) images, which requires assumptions about the third, depth dimension. Given advances in image processing, we examined how cell volumes determined from three-dimensional (3D), confocal images affected established relationships between phytoplankton cell volume and C and N content. Additionally, we determined that growth conditions could result in 30–40% variation in cellular N and C. 3D phytoplankton cell volume measurements were on average 15% greater than the geometric approximations from 2D images. Volume method variation was minimal compared to both intraspecific variation in volumes (~30%) and the 50-fold variation in elemental density among species. Consequently, C:vol and N:vol relationships were unaltered by volume measurement method and growth environment. Recent advances in instrumentation, including those for at sea and autonomous applications can

available online at academic.oup.com/plankt

be used to estimate plankton biomass directly. Going forward, we recommend instrumentation that permits species identification alongside size and shape characteristics for plankton biomass estimates.

KEYWORDS: plankton; biomass; confocal microscopy; biovolume; cell size; carbon; nitrogen

INTRODUCTION

Phytoplankton compose the base of oceanic food webs and biogeochemical cycles, making the estimation of phytoplankton elemental composition an enduring, central theme of oceanography (Redfield, 1934). Quantifying stocks of carbon (C) and nitrogen (N) in aquatic ecosystems is fundamental to parameterizing ecosystem models and understanding biogeochemical cycles. Element-to-cell volume relationships (i.e. C:vol) overcome species-specific and size-dependent properties and enable conversion of cell size to biomass for comparison among phytoplankton communities (e.g. Litchman *et al.*, 2007; Finkel *et al.*, 2010). A common method for approximating phytoplankton biomass has been to calculate cell volume from two-dimensional (2D) microscope images (Hillebrand *et al.*, 1999) and then convert volume to carbon using C:vol relationships. Several such relationships have been published based on combining empirical measurements with meta-analyses of previously published data (e.g. Strathmann, 1967; Verity and Lagdon, 1984; Verity *et al.*, 1992; Montagnes *et al.*, 1994). This approach has yielded robust relationships between geometrically determined cell volume and carbon and nitrogen contents that are valid for diverse plankton taxa ranging several orders of magnitude in size (Menden-Deuer and Lessard, 2000). Common to all these approaches is that cell volume is estimated from geometric models that approximate and simplify often complex cell shapes using linear dimensions measured from planar images (Hillebrand *et al.*, 1999; Sun and Liu, 2003). Moreover, to estimate cell volume, the third dimension representing cell depth (z-axis) is also assumed, as cell depth is typically not measurable with traditional methods.

Over the past 20 years, there has been an expansion of the methods and instrumentation used to assess phytoplankton cell size that allows for rapid analysis of large samples and samples of whole plankton communities (Reynolds *et al.*, 2010; Lombard *et al.*, 2019; Menden-Deuer *et al.*, 2020). The expansion of high-resolution imaging has been accompanied by advances in data processing, such as algorithms that estimate cell volume from 2D images (e.g. Moberg and Sosik, 2012), and computational power for algorithms like 'marching cubes' (Lorensen and Cline, 1987). A crucial breakthrough has been the development of high-throughput instrumentation that can assess plankton cell volumes in true 3D, which supports volume approximations without assumptions about cell depth or simplification of complex shapes. To our knowledge, the ability to accurately measure the true volume of a phytoplankton cell without intermediary assumptions has not been utilized to assess whether the direct measurement of cell volume affects plankton biomass estimates and ultimately, the validity of established allometric relationships.

In addition to volume measurement method, C:vol relationships may be influenced by the environment in which cells are grown. For example, nutrient stress can induce changes in lipid concentration (Shifrin and Chisholm, 1981) which affects cellular C and N content and low light can decrease phytoplankton growth rate and lead to an accumulation of cellular nitrogen (Needoba and Harrison, 2004). These studies demonstrated that change in cellular C and N due to light or nutrient conditions differed among phytoplankton groups, likely reflecting differences in physiology and metabolic capacity among phytoplankton lineages (Shifrin and Chisholm, 1981; Needoba and Harrison, 2004). However, the effect of changing environmental conditions on elemental composition of phytoplankton has not been assessed across a broad size range of taxonomically diverse phytoplankton and thus it is unclear to what degree growth conditions would alter biomass estimates from cell-volume relationships, which include many phytoplankton lineages.

Given advances in image processing, the expansion of platforms that measure cell size, and advanced understanding of factors, such as light and nutrient stress, that influence phytoplankton elemental composition, we reexamined the relationship between phytoplankton cell volume and C and N content. Our primary goal was to determine if assessment of the direct cell volume, based on 3D measurements of complex shapes, fundamentally altered estimates of C or N content, which would suggest that 3D assessments provide superior biomass estimates. We compared phytoplankton cell volumes determined from high-precision, 3D, confocal microscope images versus volumes determined from 2D images using geometric approximation. Additionally, to understand how environmental conditions affect C:vol and N:vol relationships, we quantified the nutrient content and cell volume of

cultures grown at two different light intensities over a 7-day period.

METHODS

Culture conditions

Five phytoplankton species were cultured to assess how growth condition and imaging technology affect cell-volume estimates and to quantify differences in element to volume ratios at two light intensities (species listed in Table I). Picoplankton were deliberately omitted because of their spherical shape and thus straightforward approximation of cell volume. Prior to the experiment, cultures were maintained for at least 1 year, at 15°C under cool white fluorescent lights and a 12:12 light dark cycle, at a light intensity of 100 μmol photon m^{-2} s^{-1}. The selected phytoplankton species were diverse in phylogenetic lineage, spanning three class domains and morphology, from spherical to tri-horned (Table I, Fig. 1). Cell volume of the selected phytoplankton spanned over three orders of magnitude, with cell volume ranging from ∼200 μm^3 for *Skeletonema marinoi* to ∼30000 μm^3 for *Ceratium lineatum* (Table I). Most phytoplankton cultures were grown in f/2 media without silicic acid; silicic acid was added to the medium for the diatom, *S. marinoi* (Guillard, 1975). Nutrient concentrations in the f/2 medium were in excess throughout the experimental period and we do not suspect nutrient limitation affected C or N content. Cultures were phytoplankton monospecific but xenic. Previous work has shown that antibiotics are detrimental to dinoflagellate growth and that in exponentially growing phytoplankton cultures, bacteria contribute <1% to bulk carbon and nitrogen concentrations (Menden-Deuer and Lessard, 2000). Therefore, the C and N concentrations measured from our phytoplankton cultures should at most be minimally affected by the presence of any bacteria.

Microscopy analysis

Phytoplankton cells were imaged using the confocal capabilities of the Opera Phenix High Content Screening System™ (PerkinElmer, Inc.). Confocal microscopy captures high resolution 2D images at discrete depths through an object, which enables a three-dimensional (3D) reconstruction of the object and precise measurement of the volume of the imaged object (reviewed in Amos and White, 2003). Confocal microscopy requires fluorescence for imaging, so a variety of techniques were used to label the cell walls of the phytoplankton. The thecae of dinoflagellates were stained with the fluorescent dye, Calcofluor-white, which binds to the polysaccharides in chitin and cellulose of the theca (Herth and Schnepf, 1980). The frustule (silica cell wall) of the diatom was dyed by adding PDMPO [2-(4-pyridyl)-5-((4-(2-dimethylaminoethylamino- carbamoyl)methoxy)phenyl)oxazole] (LysoSensor Yellow/Blue DND 160, Life Technologies) to the growth media, which is co-deposited with the silica frustule (Shimizu *et al.*, 2001). The outer bounds of the unarmored cells of *Hakashiwo akashiwo* were delineated by the autofluorescence from their abundant chloroplasts that abutted the cell walls.

The lag time between experimentation and imaging with the Opera Phenix microscope required cell preservation, so subsamples were preserved with glutaraldehyde (1%). Fixatives are known to cause changes in cell size (e.g. Verity *et al.*, 1992; Montagnes *et al.*, 1994; Stoecker *et al.*, 1994) with glutaraldehyde preserved cells shrinking as much as 50% or swelling as much as 30% (Menden-Deuer *et al.*, 2001), so the cell volumes reported here may be different than those of live cells. However, fixation does not alter the relative difference between imaging methods nor treatments and thus, preservation of cells did not affect our primary objective, which was to compare cell volume, carbon and nitrogen content among treatments and volume measurement methods.

Cell volume from 2D geometric approximation and directly from 3D reconstructions were both determined from images of phytoplankton cultures that were acquired from 300 μL subsamples pipetted into an optically idealized, 96-well plate (PerkinElmer CellCarrier) that was loaded directly into the Opera Phenix for imaging. Cells were imaged with a 40x or 20x water immersion objective (depending on cell size) using the Opera Phenix software, Harmony™, which handles signal detection and acquisition. After acquiring the data, images were processed in two ways. First, using Harmony™, the discrete planes from confocal images (*z*-stacks) were rendered into a 3D projection from which the software makes a measurement of the volume encompassed in the identified cell region. Second, to emulate a typical microscope image, the confocal data were converted into a maximum 2D projection which is equivalent to the view of a light microscope. The maximum projection of the confocal images enabled us to isolate the effect of 2D and 3D volumes because the exact same cells were rendered in two different ways (i.e. in 3D and in 2D using maximum projection). Additionally this aproach ensured that any differences observed in volume were not due to differences between microscopes. From the 2D projection, Harmony™ automatically identified the major and minor axis of each phytoplankton cell in the planar image. The axial measurements were then used to calculate cell volume using the geometric

Table I: Cell volume (μm^3) measured directly from 3D images, cell volume (μm^3) measured using geometric approximations and dimensions from a 2D image, cell carbon content (pg C $cell^{-1}$) and density (pg C μm^{-3}), cell nitrogen content (pg N $cell^{-1}$) and nitrogen density (pg N μm^{-3}) of the five phytoplankton species used in this study.

Species	*Skeletonema marinoi*				*Heterocapsa triquetra*				*Heterosigma akashiwo*				*Ceratium lineatum*				*Prorocentrum micans*			
Class	Bacillariophyceae				Dinophyceae				Raphidophyceae				Dinophyceae				Dinophyceae			
Geometric aprx.	Cylinder				Prolate spheroid				Sphere				Prolate spheroid				Prolate spheroid			
Sampling time	T_{24}		T_{168}		T_{24}		T_{168}		T_{24}		T_{168}		T_{24}		T_{168}		T_{24}		T_{168}	
Volume - direct 3D (μm^3)																				
High light	197	± 69	184	± 91	2602	± 640	2359	± 1015	3775	± 801	3625	± 813	30866	± 10874	27761	± 6683	18160	± 5703	30452	± 5139
Low light	177	± 71	197	± 91	2239	± 466	1929	± 314	3567	± 846	3713	± 796	27579	± 11514	23902	± 7955	24327	± NA	16760	± 4422
Volume - geometric 2D (μm^3)																				
High light	141	± 66	139	± 44	2319	± 701	1963	± 530	3217	± 924	3304	± 972	39127	± 14283	28463	± 9831	18562	± 4141	25091	± 6004
Low light	140	± 52	136	± 33	1910	± 604	1563	± 371	3008	± 848	2997	± 729	38353	± 1831	33837	± 10062	26591	± NA	14406	± 9803
C (pg C $cell^{-1}$)																				
High light	35.9	± 13.6	24.2	± 4.0	237.4	± 11.3	140.7	± 16.1	279.7	± 51.5	141.7	± 2.7	336.9	± 99.7	359.3	± 121.7	947.6	± 261.5	943.3	± 231.1
Low light	29.0	± 3.5	17.5	± 1.7	207.3	± 11.7	50.4	± 14.8	273.2	± 68.1	111.1	± 20.6	247.0	± 3.2	NA		624.6	± 80.7	612.1	± 36.4
C density (pg C μm^{-3})																				
High light	0.183	± 0.094	0.132	± 0.069	0.091	± 0.023	0.060	± 0.027	0.074	± 0.021	0.039	± 0.009	0.011	± 0.005	0.013	± 0.005	0.052	± 0.022	0.031	± 0.009
Low light	0.163	± 0.069	0.089	± 0.042	0.093	± 0.020	0.026	± 0.009	0.077	± 0.026	0.030	± 0.008	0.009	± 0.004	NA		0.026	± NA	0.037	± 0.010
N (pg N $cell^{-1}$)																				
High light	4.3	± 2.6	2.6	± 1.0	48.0	± 6.9	29.6	± 4.9	57.0	± 8.7	22.7	± 1.0	105.2	± 70.7	84.8	± 22.6	321.7	± 28.1	148.50	± 38.52
Low light	3.3	± 0.8	2.4	± 0.3	56.6	± 1.9	32.4	± 5.1	55.3	± 12.3	26.1	± 1.5	184.9	± 47.0	NA		280.3	± 38.0	381.03	± 35.61
N density (pg N μm^{-3})																				
High light	0.022	± 0.011	0.014	± 0.009	0.018	± 0.005	0.013	± 0.006	0.015	± 0.003	0.006	± 0.001	0.003	± 0.002	0.003	± 0.001	0.018	± 0.006	0.005	± 0.002
Low light	0.018	± 0.008	0.012	± 0.006	0.025	± 0.005	0.017	± 0.004	0.016	± 0.004	0.007	± 0.002	0.007	± 0.003	NA		0.012	± NA	0.023	± 0.006

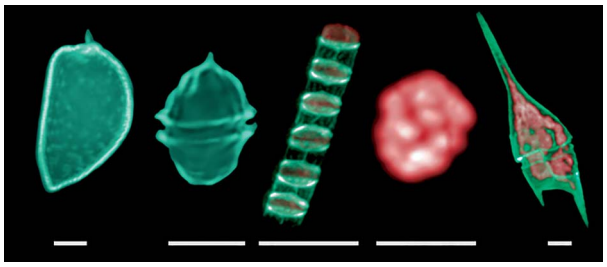

Fig. 1. Maximum projection confocal images of the five phytoplankton species used in the study. From left to right, *P. micans*, *H. triquetra*, *S. marinoi*, *H. akashiwo* and *C. lineatum*. Green fluorescence represents dyed cells, red fluorescence shows autofluorescence from chlorophyll a. All scale bars are 10 μm.

equations for a prolate spheroid, sphere or cylinder (see Table I, Hillebrand *et al.*, 1999).

Experimental conditions and elemental composition

To test the effect of light on the relationship between cell volume, and carbon and nitrogen content, exponentially growing cultures were diluted with fresh media and divided into triplicate, 1 L polypropylene bottles for high light, 100 μmol photon m^{-2} s^{-1} (HL), and low light, 15 μmol photon m^{-2} s^{-1} (LL), treatments. The LL treatment was achieved by shading the bottles in mesh bags. Bottles, containing batch cultures, for each treatment were incubated for 7 days, side by side, to minimize potential differences in temperature or light spectra. The experiment was conducted in the same 15°C, environmentally controlled incubator in which the cultures had been maintained. To assess differences in cell size and elemental quotas, subsamples were collected 24 h ($\mathcal{T}_{24}$), and 7 days (168 h) after the initiation of the experiment ($\mathcal{T}_{168}$).

Carbon and nitrogen concentrations were determined from 50 mL subsamples (except the subsample for *S. marinoi* at $\mathcal{T}_{168}$ was 25 mL, due to high density) that were filtered onto pre-combusted (500 °C for 4 h) GF/F filters and analyzed for CHN on an Exeter Analytical CE-440 elemental analyzer (URI-GSO, analytical lab). Cell abundances were enumerated from Lugol's preserved (2%) subsamples using a gridded Sedgewick-Rafter chamber and a Nikon Eclipse E800 microscope.

Data and statistical analysis

All statistical analyses were performed using R packages (R Core Team, 2019). A two-way ANOVA with species as a random variable was used to test for differences between cell-volume measurement methods. Two-way, mixed-effect ANOVAs with species as a random variable were used to assess differences in cell volume, C and N content with respect to light treatment and sampling time. ANCOVA was used to test if imaging method altered C:vol and N:vol ratios. Elemental concentration and cell volumes were normalized through $\log_{10}$ transformation before ANCOVA analysis. ANCOVA was also used to test the effects of light intensity and sampling time on the elemental to volume ratios. The relationships of C:vol and N:vol were determined using the HL cultures and model II, standard major axis linear regression. Figures show the log–log relationships between C, N and volume while equations are given in the non-log format. Note that the log format can be obtained via $y = a\ \mathrm{vol}^b \Leftrightarrow \log y = b \log \mathrm{vol} + \log a$, where b is the slope of the log regression and a is the y-intercept.

RESULTS

Cell volume spanned three orders of magnitude among species (Table I). Remarkably, the average coefficient of variation (CV) of volume was similar regardless if the measurement was made directly from the 3D image or using a 2D geometric approximation. Direct 3D volume measurement varied 28% on average and volume measurements using the 2D geometric approximation varied by 32% on average for a given species.

Comparing 3D volume to 2D geometric approximations

Overall, direct cell-volume measurements from the 3D images were significantly greater than the geometric cell volume ($P = 0.03$, one-way ANOVA with species as a random variable). However, neither method gave consistently greater or smaller volumes. Cell volume measured using the 3D image ranged from −15% smaller for *C. lineatum* to 23% greater for *S. marinoi* than the geometric cell volumes (Fig. 2). The direct 3D and geometric (2D) cell volumes were significantly different for *C. lineatum*, *H. akashiwo,* and *Prorocentrum micans* ($P < 0.001$, two-way ANOVA). The mean difference between direct 3D and 2D geometric cell volume measurements for a single species was $15 \pm 4\%$, which is half of the intraspecific variation (∼30%). All analyses presented hereafter are based on the cell volumes determined from the 3D images with error denoting standard deviation, unless otherwise stated.

Cellular carbon and nitrogen

Cellular carbon content ranged 50-fold among species, from 17.5 ± 1.7 to 948 ± 261.5 pg C $cell^{-1}$ (Table I, Fig. 3a). Cellular carbon content was significantly lower in the low light treatments ($P = 0.02$, two-way ANOVA).

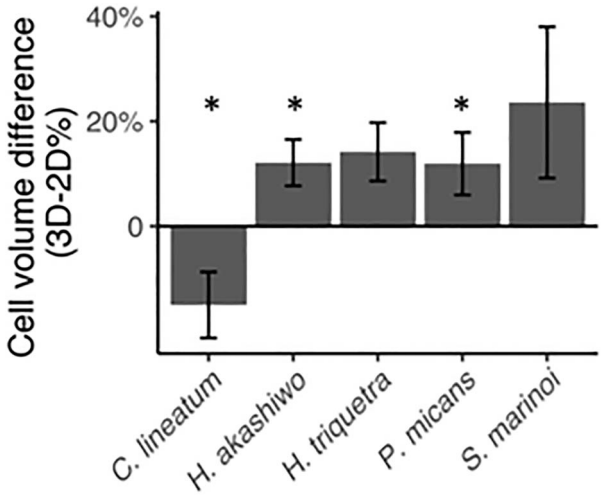

Fig. 2. Species-specific differences (%) in biovolume measured directly from 3D images and geometrically from 2D images. Asterisks demark instances where 3D volume estimate was significantly different from 2D estimate, error bars represent one standard deviation. Only the 3D volume for *C. lineatum* was less than the 2D volume.

Cells growing in low light had 30% less C cell^{-1} on average than those growing in high light. However, there was no difference between the two time points, T_{24} and T_{168} ($P = 0.15$), nor was there an interaction effect between time and light treatment. Cell volume generally decreased in the LL treatment at the final (T_{168}) timepoint (Table I). However, cell volume was not significantly affected by time or light level ($P = 0.43$ and $P = 0.94$, respectively). Carbon density ranged from 0.009 ± 0.004 to 0.183 ± 0.094 pg C μm^{-3} among species and treatments (Table I, Fig. 3b). Combined changes in C cell^{-1} and cell volume, lead to a 40% decrease in cellular C density by T_{168}. Cellular C density was significantly lower at T_{168} ($P = 0.001$) irrespective of light treatment ($P = 0.08$).

Cellular nitrogen ranged three orders of magnitude, from 2.4 ± 0.3 to 381 ± 35.6 pg N cell^{-1} among species (Table I, Fig. 3c). Cellular nitrogen did not vary systematically with light treatment ($P = 0.17$) nor sampling time point ($P = 0.27$). The nitrogen density of cells ranged from 0.003 ± 0.002 to 0.025 ± 0.005 pg N μm^{-3} (Table I, Fig. 3d). Nitrogen density had decreased roughly 30% by T_{168} and showed a significant response to sampling time ($P = 0.02$) but was not different between light treatments ($P = 0.29$).

C:Vol and N:Vol relationships and the effect of imaging, light and time

Despite as much as a 23% difference in volume for a given species, using cell volume determined from a geometric approximation or directly from a 3D images did not affect the relationship of C:vol ($P = 0.70$, one-way ANOVA) or N:vol ($P = 0.62$; Fig. 4). Although our sample size was not intended to establish allometric relationships, the data obtained here compare favorably to prior analyses. The element-to-volume relationships did not differ based on light conditions (C:vol, $P = 0.28$ and N:vol, $P = 0.24$) nor sampling time (C:vol, $P = 0.13$ and N:vol, $P = 0.11$). Thus, the overarching relationships based on the directly measured 3D volumes with all light and time data, yielded: pg C cell$^{-1} = 0.735$ x vol$^{0.664}$ and pg N cell$^{-1} = 0.034$ x vol$^{0.866}$ (Fig. 4). The exponent (i.e. slope of the log–log regression) of the C relationship was significantly lower than Menden-Deuer and Lessard (2000) 0.819, ($P = 0.01$) however, if *C. lineatum* was excluded, which had relatively low C cell^{-1}, the exponent became, 0.746 which was not significantly different from Menden-Deuer and Lessard (2000) ($P = 0.11$). The exponent of the N:vol relationship was not significantly different ($P = 0.60$) from the 0.849 exponent in Menden-Deuer and Lessard (2000).

The C and N density of phytoplankton cells was inversely related to cell volume (Fig. 5). Larger cells were less C dense, pg C μm$^{-3} = 2.3$ x vol$^{-0.476}$, ($P < 0.001$, Model II) and less N dense pg N μm$^{-3} = 0.19$ x vol$^{-0.345}$, ($P = 0.02$, Model II). These relationships of C and N density with cell volume were not significantly altered by light intensity ($P = 0.28$ for C, $P = 0.24$ for N) or sampling time ($P = 0.13$ for C, $P = 0.11$ for N).

DISCUSSION

The immense diversity of phytoplankton span nine orders of magnitude in cell volume (Finkel *et al.*, 2010) and encompasses morphology from simple spheres to complex shapes like the tri-horned, concave, *Ceratium* (Roselli *et al.*, 2015). Historically, microphytoplankton cell volume has been calculated using geometric approximations of cell shape based on linear measurements from 2D images (Hillebrand *et al.*, 1999; Sun and Liu, 2003). Here, we show that C and N element-to-cell volume relationships were not altered by high precision, direct measurements of cell volume nor growth condition. Elemental composition can be determined reliably, irrespective of which volume measurement method was used and to what growth condition the phytoplankton were subjected.

Element-to-volume relationships

The differences observed due to the method used to estimate volume and growth condition were minor (15–40%), in comparison to the large differences in volume (three orders of magnitude) and elemental composition (50-fold) among phytoplankton species that

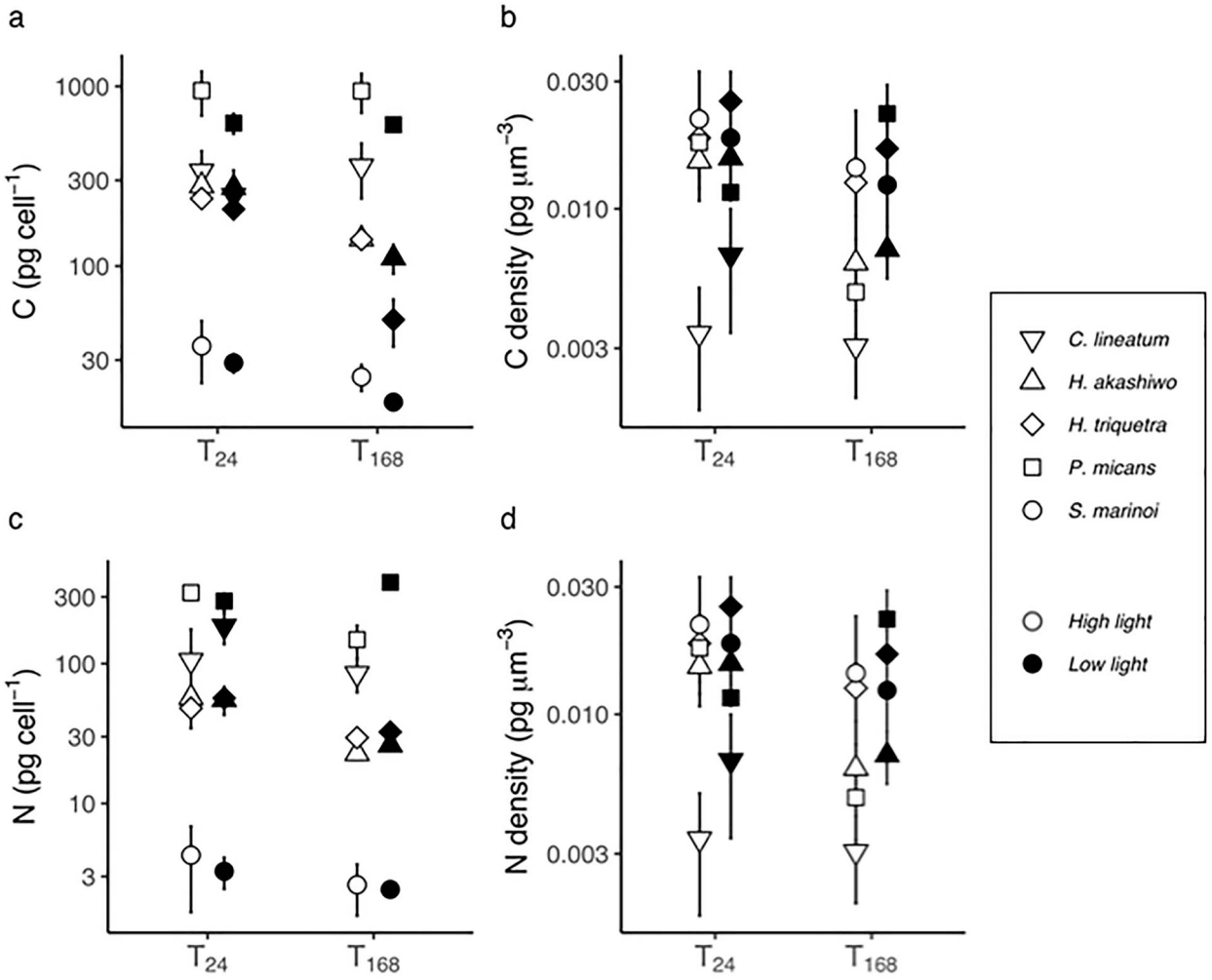

Fig. 3. (a) Cellular C (pg C cell^{-1}), (b) C density (pg C µm^{-3}), (c) Cellular N (pg N cell^{-1}) and (d) N density (pg C µm^{-3}) of species during the experiment at each time point. High-light and low-light growth conditions are indicated with white and black symbols, respectively. Note log scaled *y*-axes. Shapes of points correspond to phytoplankton species and error bars represent one standard deviation. Data without error bars have standard deviation within the height of the symbol.

are included in allometric relationships. Thus, given both biological and methodological variation across instrument platforms that use a range of methods to estimate cell volume (Reynolds *et al.*, 2010; Menden-Deuer *et al.*, 2020), the established C:vol and N:vol relationships can reasonably be applied to estimate elemental composition of phytoplankton stocks.

The minimal effect of growth environment on the relationship between cell volume and C and N is consistent with global assessments of phytoplankton stoichiometry, where changes in the elemental composition of phytoplankton are primarily influenced by community composition (Twining *et al.*, 2011; Weber and Deutsch, 2012; Martiny *et al.*, 2013) and to a much lower extend by environment (Twining *et al.*, 2011). The dominance in taxonomy as a driver of elemental composition stresses the need for continued and persistent assessment of species identity (Menden-Deuer and Kiørboe, 2016) alongside ecological and physiological characteristics, for biomass assessments and in general.

Biovolume estimates

There are a few reasons why the direct 3D volume differed from geometric approximation. First, cells imaged using the Opera Phenix were suspended in liquid media, in a 96 well plate. For the 3D image, cell orientation is irrelevant to the volume measurement because all three dimensions are captured. However, in a 2D image any orientation of the cell that is not perpendicular to the objective will result in a relatively shortened measurement of the major or minor axis and thus cause an underestimate of cell

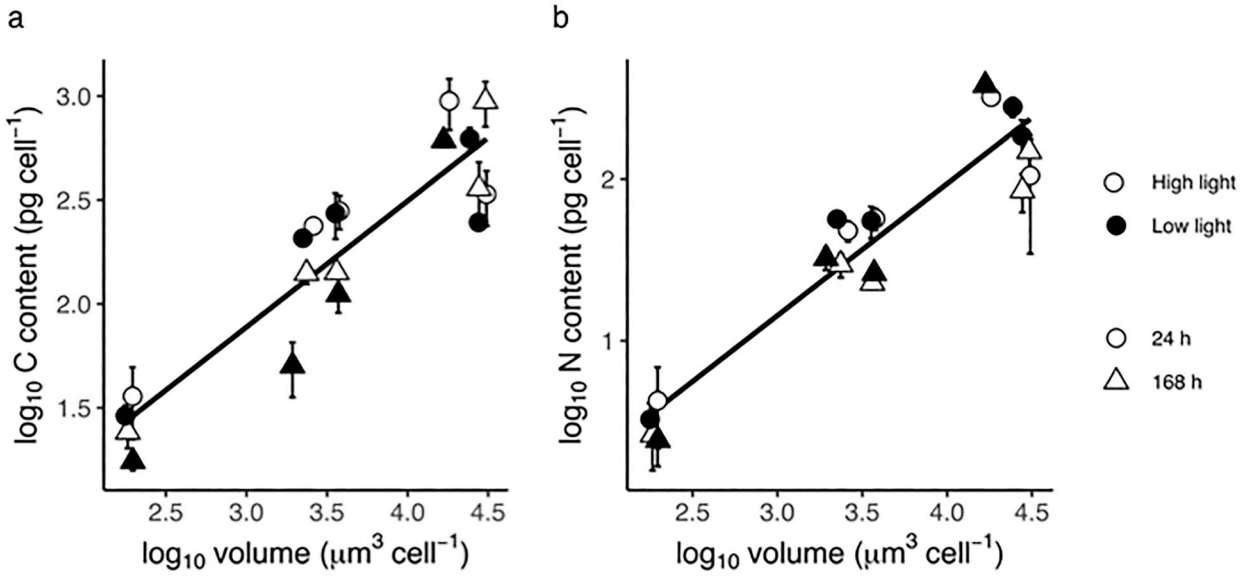

Fig. 4. The relationship between phytoplankton volume (μm^3 $cell^{-1}$) and (a) carbon content (pg C $cell^{-1}$) and (b) nitrogen content (pg N $cell^{-1}$). Error bars represent one standard deviation. Neither light intensity (white versus black) nor time of sampling (circles versus triangles) significantly altered relationships.

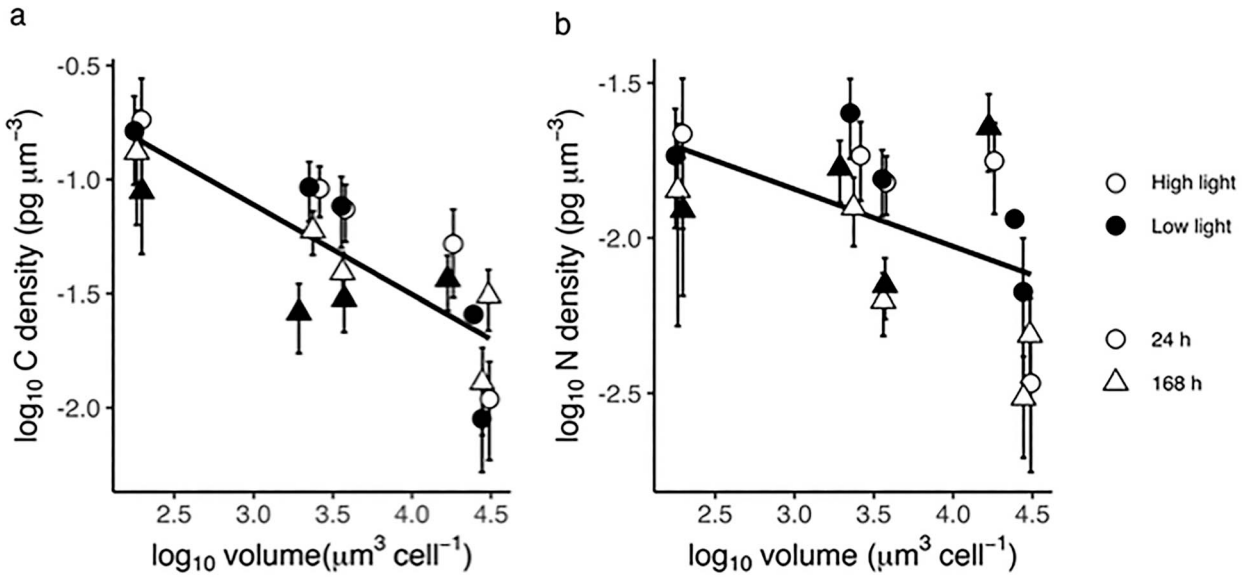

Fig. 5. The relationship between phytoplankton volume and (a) carbon density (pg C μm^{-3}) and (b) nitrogen density (pg N μm^{-3}). Error bars represent one standard deviation. Neither light intensity (white versus black) nor time of sampling (circle versus triangle) significantly altered allometric relationships.

volume. Second, the differences between the direct 3D and geometric volumes arise from the simplification of complex cell shapes and the necessary assumptions made about the *z*-axis (depth) in a 2D image. The simplification of complex shapes would tend to make the direct 3D volume less than the geometric volume (Roselli *et al.*, 2013, 2015). However, in all but one of the species examined the direct 3D volume was greater than the geometric volume. In our geometric volume estimate, we assumed that the *z*-depth of the cell was equal to the minor axis in the planar view. To bring the direct 3D and geometric (2D) volume measurements into agreement, the *z*-axis would have to be 20% longer that the planar-view minor axis. For example, for a cell with a minor axis of 15 μm, the increase

in the *z*-axis would be 3 μm, which would be within measurement error of standard microscopy. However, because cells generally settle with the shortest dimension in the *z*-direction, it is more probable that the differences between volume estimates were due to cell orientation.

Confocal microscopy produces high-resolution images that enable high-precision cellular measurements (e.g. Roselli *et al.*, 2013, 2015), yet there are tradeoffs of time and accessibility. High-resolution confocal images take roughly two-to-three times as much time to acquire and analyze than those from a standard microscope. Additionally, while epifluorescence microscopes are relatively common instrumentation in microbial labs, confocal microscopes are rarer and often harder to access. Thus, confocal microscopy is a powerful instrument when interrogating detailed cell physiology, but we find the higher resolution capabilities, which result in an ∼15% difference in volume estimates, do not provide sufficient advancement to justify the effort and do not deem this application necessary when estimating carbon content of phytoplankton that span orders of magnitude in size.

Growth conditions

Consistent with other studies (e.g. Needoba and Harrison, 2004; Twining *et al.*, 2011), we see evidence of altered elemental concentrations among cells that were subjected to different growth environments. Also consistent with previous findings, these responses varied among species (Shifrin and Chisholm, 1981; Needoba and Harrison, 2004; Twining *et al.*, 2011). Our results show that both the magnitude and direction of change in elemental cell concentration varied between species. For example, some cells had higher N content, thus higher N density under low-light conditions while others became less N dense. Species, or group-specific, responses to a changing environment are expected and result from diverse metabolic strategies among phytoplankton (Stehfest *et al.*, 2005; Alexander *et al.*, 2015). Despite differences among species, C and N density decreased overall by the final sampling point. Cellular nutrient density can change due to nutrient stress (e.g. Shifrin and Chisholm, 1981), though nutrient limitation seems unlikely in this instance given the use of f/2 media. Specifically, since the experiment was initiated with a 50% dilution the minimum concentration of nitrate would have been 440 μM. The most prolific of the phytoplankton, *S. marinoi*, grew to a biomass of 100 μM of particulate nitrogen by T_{168} suggesting that ∼300 μM nitrate remained in the growth medium. As such, the underlying mechanism leading to the decrease in N and C density is unclear. One possibility is a reduction in growth rate and a commensurate reduction in nutrient storage.

While our results suggest that growth environment would not significantly change estimates of phytoplankton carbon and nitrogen stock, changes in light and nutrient availability can have ecosystem consequences. For example, nutrient stress can change cell amino acid and lipid composition resulting in higher C:N ratios (Stehfest *et al.*, 2005) which may alter ecosystem processes such as nutrient assimilation by zooplankton (Van Donk *et al.*, 1997) or phytoplankton sinking speed (Waite and Nodder, 2001). Thus, growth environment likely plays an important role in altering the fate of phytoplankton biomass.

CONCLUSION AND RECOMMENDATIONS

Biomass estimates based on phytoplankton cell volume and established C and N content were minimally altered based on growth environment or by methodological differences in measuring cell volume. Thus, we suggest that established broad-scale, cross-taxa elemental ratio relationships provide reasonable approximations of cellular C and N content (Menden-Deuer and Lessard, 2000) and do not see a necessity for reevaluation of allometric relationships based on 3D measurements of cell volume. The over-representation of some phylogenetic groups (e.g. diatoms) in allometric relationships relative to others that are still missing (e.g. ciliates) remains a problem. The increased precision of measuring cell volume directly with 3D imaging techniques (Roselli *et al.*, 2013) did not substantially change relationships between cell volume and elemental content, which were determined using phytoplankton species that differ by orders of magnitude in size. Thus, we recommend that the procedures outlined in Menden-Deuer and Lessard (2000) are reliable for estimating plankton biomass and we see no need for either a revision of historic time series data or a community wide effort to adopt new measurement techniques. Going forward, we recommend a focus on instrumentation that permits both species identification alongside size and shape characteristics for plankton biomass estimates, particularly to utilize *in situ*, autonomous observation capabilities (e.g. Olson and Sosik, 2007).

ACKNOWLEDGEMENTS

Thank you to V. Craver (VOC) and her support through the use of the Opera Phenix™. A special thank you to the GSO REU program directors, L. Maranda and D. Smith. Thank you to R.P. Kelly for facilitating CHN analysis.

FUNDING

National Aeronautics and Space Administration (80NSSC17K0716 to S.M.D.); National Science Foundation (OCE-1736635 to S.M.D.); National Science Foundation (CBET-1828057 to V.O.C.). C.N. Hammond was supported by the National Science Foundation, Research Experience for Undergraduate fellowship at the University of Rhode Island, award OCE-1757572.

REFERENCES

Alexander, H., Jenkins, B. D., Rynearson, T. A. and S. T. Dyhrman. (2015) Metatranscriptome analyses indicate resource partitioning between diatoms in the field. *Proc. Natl. Acad. Sci.*, **112**, E2182–E2190.

Amos, W. B. and White, J. G. (2003) How the confocal laser scanning microscope entered biological research. *Biol. Cell*, **95**, 335–342.

Finkel, Z. V, J. Beardall, K. J. Flynn, A. Quigg, T. A. V Rees, and J. A. Raven. (2010) Phytoplankton in a changing world: cell size and elemental stoichiometry. *J. Plankton Res.*, **32**, 119–137.

Guillard, R. R. L. (1975). Culture of Phytoplankton for Feeding Marine Invertebrates. In *Culture of Marine Invertebrate Animals* (pp. 29–60). Springer US. https://doi.org/10.1007/978-1-4615-8714-9_3

Herth, W. and Schnepf , E. (1980) The fluorochrome, calcofluor white, binds oriented to structural polysaccharide fibrils. *Protoplasma*, **105**, 129–133.

Hillebrand, H., C.-D. Dürselen, D. Kirschtel, U. Pollingher, and T. Zohary. (1999) Biovolume calculation for pelagic and benthic microalgae. *J. Phycol.*, **35**, 403–424.

Litchman, E., C. A. Klausmeier, O. M. Schofield, and P. G. Falkowski. (2007) The role of functional traits and trade-offs in structuring phytoplankton communities: scaling from cellular to ecosystem level. *Ecol. Lett.*, **10**, 1170–1181.

Lombard, F., Boss, E., Waite, A.M., Vogt, M., Uitz, J., Stemmann, L. Sosik, H.M., Shulz, J. *et al.* (2019) Globally consistent quantitative observations of planktonic ecosystems. *Front. Mar. Sci.*, **6**, 196.

Lorensen, W. E. and Cline, H. E. (1987) Marching cubes: a high resolution 3D surface construction algorithm. *Proc. 14th Annu. Conf. Comput. Graph. Interact. Tech. SIGGRAPH* **1987**, 21, 163–169.

Martiny, A. C., C. T. A. Pham, F. W. Primeau, J. A. Vrugt, J. K. Moore, S. A. Levin, and M. W. Lomas. (2013) Strong latitudinal patterns in the elemental ratios of marine plankton and organic matter. *Nat. Geosci.*, **6**, 279–283.

Menden-Deuer, S., E. Lessard, and J. Satterberg. (2001) Effect of preservation on dinoflagellate and diatom cell volume, and consequences for carbon biomass predictions. *Mar. Ecol. Prog. Ser.*, **222**, 41–50.

Menden-Deuer, S., Morison, F., Montalbano, A.L., Franze, G., Strock, J., Rubin, E., McNair, H. M., Mouw, C., *et al.* (2020) Multi-instrument assessment of phytoplankton abundance and cell sizes in monospecific laboratory cultures and whole plankton community composition in the North Atlantic. *Front. Mar. Sci.*, **7**, 1–14.

Menden-Deuer, S. and Kiørboe, T. (2016) Small bugs with a big impact: linking plankton ecology with ecosystem processes. *J. Plankton Res.*, **38**, 1036–1043.

Menden-Deuer, S. and Lessard, E. J. (2000) Carbon to volume relationships for dinoflagellates, diatoms, and other protist plankton. *Limnol. Oceanogr.*, **45**, 569–579.

Moberg, E. A. and Sosik, H. M. (2012) Distance maps to estimate cell volume from two-dimensional plankton images. *Limnol. Oceanogr. Methods*, **10**, 278–288.

Montagnes, D. J. S., J. A. Berges, P. J. Harrison, and F. J. R. Taylor. (2001) A novel fuorescent silica tracer for biological silicication studies. *Chem. Biol.*, **8**, 1051–1060.

Needoba, J. A. and Harrison, P. J. (2004) Influence of low light and a light: dark cycle on NO3- uptake, intracellular NO3-, and nitrogen isotope fractionation by marine phytoplankton. *J. Phycol.*, **40**, 505–516.

Olson, R. J. and Sosik, H. M. (2007) A submersible imaging-in-flow instrument to analyze nano-and microplankton: imaging FlowCytobot. *Limnol. Oceanogr. Methods*, **5**, 195–203.

R Core Team (2019) R: A language and environment for statistical computing. R Foundation for Statistical Computing, Vienna, Austria. URL https://www.R-project.org/.

Redfield, A. C. (1934) *On the Proportions of Organic Derivatives in Sea Water and Their Relation to the Composition of Plankton*, James Johnson Memorial Volume. University of Liverpool, Liverpool, pp. 177–192.

Reynolds, R. A., D. Stramski, V. M. Wright, and S. B. Woźniak (2010) Measurements and characterization of particle size distributions in coastal waters. *J. Geophys. Res. Ocean.*, 115.

Roselli, L., E. Stanca, F. Paparella, A. Mastrolia, and A. Basset. 2013. Determination of Coscinodiscus cf. granii biovolume by confocal microscopy: comparison of calculation models. *J. Plankton Res.*, **35**, 135–145.

Roselli, L., F. Paparella, E. Stanca, and A. Basset (2015) New data-driven method from 3D confocal microscopy for calculating phytoplankton cell biovolume. *J. Microsc.*, **258**, 200–211.

Shifrin, N. S. and Chisholm, S. W. (1981) Phytoplankton lipids: interspecific differences in the effects of nitrate, silicate and light-dark cycles. *J. Phycol.*, **17**, 374–384.

Shimizu, K., Y. Del Amo, M. A. Brzezinski, G. D. Stucky, and D. E. Morse. (1994) Estimating carbon, nitrogen, protein, and chlorophyll a from volume in marine phytoplankton. *Limnol. Oceanogr.*, **39**, 1044–1060.

Stehfest, K., J. Toepel, and C. Wilhelm. (2005) The application of micro-FTIR spectroscopy to analyze nutrient stress-related changes in biomass composition of phytoplankton algae. *Plant Physiol. Biochem.*, **43**, 717–726.

Stoecker, D. K., D. J. Gifford, and M. Putt. (1994) Preservation of marine planktonic ciliates: losses and cell shrinkage during fixation. *Mar. Ecol. Prog. Ser.*, **110**, 293–299.

Strathmann, R. R. (1967) Estimating the organic carbon content of phytoplankton from cell volume or plasma volume. *Limnol. Oceanogr.*, **12**, 411–418.

Sun, J. and Liu, D. (2003) Geometric models for calculating cell biovolume and surface area for phytoplankton. *J. Plankton Res.*, **25**, 1331–1346.

Twining, B. S., S. B. Baines, J. B. Bozard, S. Vogt, E. a. Walker, and D. M. Nelson. (2011) Metal quotas of plankton in the equatorial Pacific Ocean. *Deep. Res.* **Part II**, 58, 325–341.

Van Donk, E., Lurling, M., Hessen, D. O., and G. M. Lokhorst. (1997) Altered cell wall morphology in nutrient-deficient phytoplankton and its impact on grazers. *Limnol. Oceanogr.*, **42**, 357–364.

Verity, P. G., C. Y. Robertson, C. R. Tronzo, M. G. Andrews, J. R. Nelson, and M. E. Sieracki. (1992) Relationships between cell volume and the carbon and nitrogen content of marine photosynthetic nanoplankton. *Limnol. Oceanogr.*, **37**, 1434–1446.

Verity, P. G. and Lagdon, C. (1984) Relationships between lorica volume, carbon, nitrogen, and ATP content of tintinnids in Narragansett Bay. *J. Plankton Res.*, **6**, 859–868.

Waite, A. and Nodder, S. D. (2001) The effect of in situ iron addition on the sinking rates and export flux of Southern Ocean diatoms. *Deep. Res. II*, **48**, 2635–2654.

Weber, T. and Deutsch, C. (2012) Oceanic nitrogen reservoir regulated by plankton diversity and ocean circulation. *Nature*, **489**, 419–422.